Reversible effect of strain on transport critical current in $Bi_2Sr_2CaCu_2O_{8+x}$ superconducting wires: a modified descriptive strain model



2012 Supercond. Sci. Technol. 25 015001

(http://iopscience.iop.org/0953-2048/25/1/015001)

Supercond. Sci. Technol. **25** (2012) 015001 (16pp) doi:10.1088/0953-2048/25/1/015001

# Reversible effect of strain on transport critical current in $Bi_2Sr_2CaCu_2O_{8+x}$ superconducting wires: a modified descriptive strain model*

**N Cheggour[1,2], X F Lu[1,2], T G Holesinger[3], T C Stauffer[1], J Jiang[4] and L F Goodrich[1]**

[1] Electromagnetics Division, National Institute of Standards and Technology, Boulder, CO 80305, USA
[2] Department of Physics, University of Colorado, Boulder, CO 80309, USA
[3] Superconductivity Technology Center, Los Alamos National Laboratory, Los Alamos, NM 87545, USA
[4] Applied Superconductivity Center, National High Magnetic Field Laboratory, Florida State University, Tallahassee, FL 32310, USA

E-mail: cheggour@boulder.nist.gov

Received 8 July 2011, in final form 19 October 2011
Published 5 December 2011
Online at stacks.iop.org/SUST/25/015001

**Abstract**
A reversible strain effect on transport critical current $I_c$ was found in $Bi_2Sr_2CaCu_2O_{8+x}$ (Bi-2212) high-temperature superconducting round wires. $I_c$ showed unambiguous reversibility at 4 K and 16 T up to an irreversible strain limit of about 0.3 % in longitudinal tension, prompting hope that the Bi-2212 conductor has the potential to sustain mechanical strains generated in high-field magnets. However, $I_c$ was not reversible under longitudinal compression and buckling of Bi-2212 grain colonies was identified as the main reason. A *two-component model* was proposed, which suggests the presence of mechanically weak and strong Bi-2212 components within the wire filaments. Porosity embedded in the weak component renders it structurally unsupported and, therefore, makes it prone to cracking under strain $\varepsilon$. $I_c(\varepsilon)$ is irreversible in tension if the weak component contributes to the transport critical current but becomes reversible once connectivity of the weak component is broken through strain increase or cycling. A *modified descriptive strain model* was also developed, which illustrates the effect of strain in the Bi-2212 conductor and supersedes the existing descriptive model. Unlike the latter, the new model suggests that higher pre-compressive strains should improve $I_c$ if buckling of Bi-2212 grains does not occur, and should result in a wider $I_c(\varepsilon)$ plateau in the applied tensile regime without degradation of the initial $I_c$. The new model postulates that a reversible strain effect should exist even in the applied compressive strain regime if buckling of Bi-2212 grains could be prevented through elimination of porosity and mechanical reinforcement of the wire.

## 1. Introduction

Development of superconducting magnets capable of generating fields significantly beyond 20 T necessitates the use of cuprate superconductors [1–4]. Whereas $Nb_3Sn$ exhibits intrinsic limitations and insufficient flux pinning at high magnetic fields [5], Bi–Sr–Ca–Cu–O and Y–Ba–Cu–O superconductors show high critical current density $J_c$ in fields past 20 T [6] and still have a wide margin for further improvement.

* Contribution of NIST, an agency of the US government, not subjected to copyright.

 

The $Bi_2Sr_2Ca_1Cu_2O_{8+x}$ material, commonly referred to as Bi-2212, can be made into a round-wire conductor. This unique feature amongst the cuprate superconductors—which otherwise can be fabricated only into a tape-conductor form so far—makes the Bi-2212 strand particularly suitable for magnet technology. Undeniably, Bi-2212 round wires can be wound easily to fabricate solenoid magnets and can be used to produce Rutherford cables needed for dipole and quadrupole magnets [7–9].

Albeit this feature is attractive, alone it is not sufficient. Higher values of $J_c$ and better resilience to mechanical strain are also required to make the Bi-2212 technology more reliable for magnet applications such as high-energy-physics particle accelerators and nuclear magnetic resonance (NMR) spectroscopy.

In this paper, we focus on the electromechanical properties of Bi-2212 conductors. We review some of the most significant literature on this topic and the current understanding of the strain effects in Bi-2212. We also investigate a recently developed Bi-2212 wire and formulate a new perception of the effect of strain in this material.

## 2. Background of the strain effect in Bi-2212 conductors

Bi-2212 strands are known to show irreversible degradation of their critical current $I_c$ when subjected to applied tensile or compressive axial strain $\varepsilon$ [10–14]. It is also commonly agreed that the behavior of $I_c(\varepsilon)$ in Bi-2212 wires and tapes is extrinsic in nature, governed by mechanical fractures of the brittle Bi-2212 material [10–14]. Interestingly, however, ten Haken *et al* observed, by use of x-ray diffraction, an elastic deformation of the Bi-2212 grains along the *c* axis when small strains were applied at room temperature to a polycrystalline Bi-2212 tape [15]. The strain range of this elastic deformation was between $-0.1\%$ and $+0.2\%$. Nonetheless, due to the irreversible nature of $I_c(\varepsilon)$, ten Haken *et al* concluded that this elastic deformation of the lattice does not change $I_c$, and that the small and irreversible change of $I_c$ within the elastic strain range is due to micro-cracks of the material along its grain boundaries [14]. Later on, ten Haken *et al* remarked that $I_c$ in $Bi_2Sr_2Ca_2Cu_3O_{10+x}$ (Bi-2223; which arguably has a similar mechanical behavior to the Bi-2212 system) showed a partial recovery when strain is released from small tensile values, which indicated a certain reversible strain behavior in Bi-2223 material that coexisted with a predominantly irreversible degradation [16]. Thereafter, Sugano and Osamura discovered a clear reversible strain effect in Bi-2223 composite tapes [17, 18]. To our knowledge, nevertheless, a reversible strain effect has not been reported in Bi-2212 conductors.

A descriptive model for the irreversible reduction of $I_c$ with strain in Bi-2212 conductors was developed by ten Haken *et al* [14]. It assumes that the highest $I_c$ value—but unobtainable in a composite—is when the Bi-2212 material is in a strain-free state and not surrounded by a matrix (see figure 2 of [14]). The model states that the pre-compression that is exerted on Bi-2212 by its surrounding matrix during the sample cool-down to an operating cryogenic temperature drives $I_c$ to a lower value following the same, mostly linear, dependence of $I_c$ on axial compressive mechanical strain [12, 14]. According to the descriptive model, application of a tensile strain to the sample after cool-down does not bring $I_c$ back up due to the lack of a reversible strain effect in this material. Rather, $I_c$ remains almost unchanged or decreases slightly until a certain critical strain is reached that fully compensates for the pre-compressive strain that Bi-2212 was subjected to after cool-down. Beyond this strain, a precipitous drop in $I_c$ occurs.

Management of stress and strain is particularly crucial in high-field and large-size magnets in order to overcome the significant thermal and mechanical constraints on the conductor during magnet cool-down and operation. The observed irreversible behavior of $I_c$ with strain in Bi-2212 strands could make the design of a magnet difficult and its performance potentially unpredictable. Therefore, it is important to fully understand the effect of strain and its origins in Bi-2212 material.

In this paper, we re-examine the strain effect in Bi-2212 wires. We show that $I_c$ can actually exhibit a reversible behavior with applied tensile strain. This finding prompts hope that there may be a useful strain window for safely operating magnets made of Bi-2212 conductors. We discuss this reversibility and propose a model to explain why it disappears in some samples and under certain conditions. In light of this new understanding, we also formulate a modified descriptive strain model to elucidate the behavior of Bi-2212 wires with strain. These proposed models are corroborated with a microscopic investigation of the microstructure of the strained samples.

## 3. Samples investigated and heat treatment

The Bi-2212 wire investigated had 18 bundles of 37 filaments each ($37 \times 18$ design). It was fabricated by Oxford Superconductor Technology (OST; billet number PPM091221-2) by use of the powder-in-tube (PIT) process [19]. Precursor powder used in the wire manufacturing was granular powder made by Nexans. The filaments were surrounded by a pure Ag matrix and the wire had an external reinforcing sheath made of Ag–0.2 wt%Mg alloy. The wire diameter was 0.8 mm.

Pieces of this wire, each approximately 2 m long, were wound on heat-treatment mandrels made of a machinable alumina and heat-treated at Florida State University (FSU) and Los Alamos National Lab (LANL). The heat treatment was a partial-melt process [20] performed at a temperature of 888 °C. Nevertheless, several details of the heat-treatment schedules used by FSU and LANL were significantly different. In particular, the dwell time at the highest temperature—time in the melt [21, 22]—was 30 min at LANL and only 12 min at FSU. Parameters of the two heat treatments are given below.

Heat-treatment schedule used at FSU: ramp up at 160 °C $h^{-1}$ from room temperature directly to 830 °C and dwell for 5 h; ramp up at 50 °C $h^{-1}$ to 888 °C and dwell for 0.2 h; ramp down at 10 °C $h^{-1}$ to 878 °C; ramp down at 2.5 °C $h^{-1}$ to 836 °C and hold for 48 h; then ramp down at 80 °C $h^{-1}$ to room temperature.

Heat-treatment schedule used at LANL: ramp up at 100 °C $h^{-1}$ from room temperature to 150 °C and dwell for 2 h; ramp up at 100 °C $h^{-1}$ to 400 °C and dwell for 5 h; ramp up at 100 °C $h^{-1}$ to 850 °C and dwell for 25 h; ramp up at 50 °C $h^{-1}$ to 888 °C and dwell for 0.5 h; ramp down at 10 °C $h^{-1}$ to 878 °C and hold for 0.1 h; ramp down at 2 °C $h^{-1}$ to 835 °C and dwell for 60 h; ramp down at 60 °C $h^{-1}$ to 700 °C and hold for 5 h; then ramp down at 60 °C $h^{-1}$ to room temperature.

Samples investigated will be referred to with a nomenclature containing the acronym of the institute where the heat treatment was performed, followed by the sample number. For example, LANL-1 and FSU-3 will identify samples #1 and #3 of those processed at LANL and FSU, respectively.

## 4. Measurement techniques

### *4.1. Critical current and n-value measurements*

The apparatus for measuring $I_c(\varepsilon)$ utilizes a Walters' spring device for applying axial strain to the sample [23, 24]. The spring is made of cold-worked and precipitate-hardened Cu–2%Be alloy [24]. Sugano *et al* evaluated the differential thermal contraction between a typical Bi-2212 composite and Cu–Be material from room temperature to 5 K to be only about −0.01%, which indicated that the thermal contractions of the two materials do match extremely well [25]. In this type of strain experiment, where the Bi-2212 specimen is soldered to the spring, it is useful to minimize the contribution of the sample holder to the pre-compression of the specimen during cool-down. This is particularly pertinent to the Bi-2212 conductor, because of its high sensitivity to, and irreversible damage from, even small amounts of applied compressive axial strains [12, 14, 26]. Furthermore, the monotonic character of $I_c(\varepsilon)$ behavior of this material in the tensile strain regime before failure, unlike the $Nb_3Sn$ compound, for example, would make it hard to pin down the intrinsic strain tolerance of the Bi-2212 conductor under investigation if its natural pre-compressive strain is altered by the sample holder. Hence, the excellent match of the thermal contraction of the Cu–Be and Bi-2212 composite makes Cu–Be alloy the material of choice for this strain experiment [25].

The Cu–Be spring had four active turns and a T-section design that maximizes its elastic strain range to a wide window from −1% to +1% [23]. Each heat-treated Bi-2212 sample was carefully transferred from the alumina mandrel onto the spring and soldered to it at ≈200 °C with a Pb–Sn solder. Three pairs of voltage taps were attached to the sample, allowing measurement of three segments of each specimen. Each pair covered one full turn ≈8 cm long.

The relatively long separation of voltage taps made it possible to determine $I_c$ at electric-field criteria $E_c$ as low as 0.01 $\mu$V $cm^{-1}$. This enhanced the measurement sensitivity, especially in the case of Bi-2212 material, for which most of the $I_c(\varepsilon)$ data reported so far utilized $E_c$ values of 1 $\mu$V $cm^{-1}$ and higher [10–15, 25]. All $I_c$ data presented herein were determined at $E_c = 0.1$ $\mu$V $cm^{-1}$, but the electrical field $E$ versus current density $J$ curves were measured down to $E_c$ values lower than 0.01 $\mu$V $cm^{-1}$. The $n$-value, which denotes the steepness of $E$ versus $J$, was estimated for a small portion of the $E$–$J$ curve, typically between 0.07 and 0.2 $\mu$V $cm^{-1}$, centered around an $E_c$ of 0.1 $\mu$V $cm^{-1}$.

Measurements were made in liquid helium at 4.0 K. Magnetic field $B$ was supplied by a superconducting solenoid. The field and current were oriented such that the magnetic Lorentz force on the sample was directed inwards so that the sample was protected against it by the thick coiled spring. First, $I_c$ and $n$-value were measured as a function of $B$ from self-field to a maximum field of either 5 or 16 T. Thereafter, measurements of $I_c$ versus $\varepsilon$ and $n$-value versus $\varepsilon$ were carried out to examine irreversibility under tensile or compressive strain. The estimated uncertainty due to random effects in estimating critical strains was ±0.02% strain.

### *4.2. Microstructure investigation*

The microstructure of strained and unstrained samples was investigated to find a possible correlation between the sample's microstructure and its response to strain. This study was conducted at LANL by use of scanning electron microscopy (SEM). Both transverse and longitudinal cross sections of the wire were examined. Samples, which consist of wire sections about 5 mm long cut out from the coiled specimens either before or after strain measurements, were positioned in cups filled with low-viscosity epoxy and put inside a vacuum desiccator to evacuate trapped air within the sample fixture. Samples were then placed in a pressure vessel and pressurized to ≈6.9 MPa (1000 psi) to force epoxy from the sample ends into the pores present in the Bi-2212 filaments. Samples were left under pressure overnight and then heat-treated at 100 °C for 2 h to finish the curing process. Thereafter, samples were ground and polished, with the final polish made in colloidal silica. The forcing of epoxy into the pores in the specimen was necessary to provide structural protection to the Bi-2212 component during the polishing phase. After polishing, an etch of ammonium hydroxide and peroxide (1:1) diluted 50% with methanol was applied to the samples for a few seconds to remove a small amount of silver and expose the Bi-2212 filaments. Examinations of the samples' microstructure were carried out in an SEM equipped with an energy-dispersive spectrometer (EDS). The procedure for preparing samples for this study resulted in minimal residual mechanical damage to the specimens. The observed cracks and defects are strongly believed to be an integral part of the microstructure of the samples investigated, and not due to the method of sample preparation. Hence, correlations between the specimen's microstructure and its strain history could confidently be made.

## 5. Results

### *5.1. Critical current and n-value dependences on magnetic field*

Figure 1 compares $I_c(B)$ and $n$-value($B$) in ascending $B$ from self-field to 16 T, at 4.0 K and zero applied strain, for samples LANL-1 and FSU-1. The engineering critical current density $J_e$ at 16 T is close to 225 A $mm^{-2}$ at 0.1 $\mu$V $cm^{-1}$ (and 260 A $mm^{-2}$ at 1 $\mu$V $cm^{-1}$), which indicates that this wire's performance is moderately good in comparison to that of other

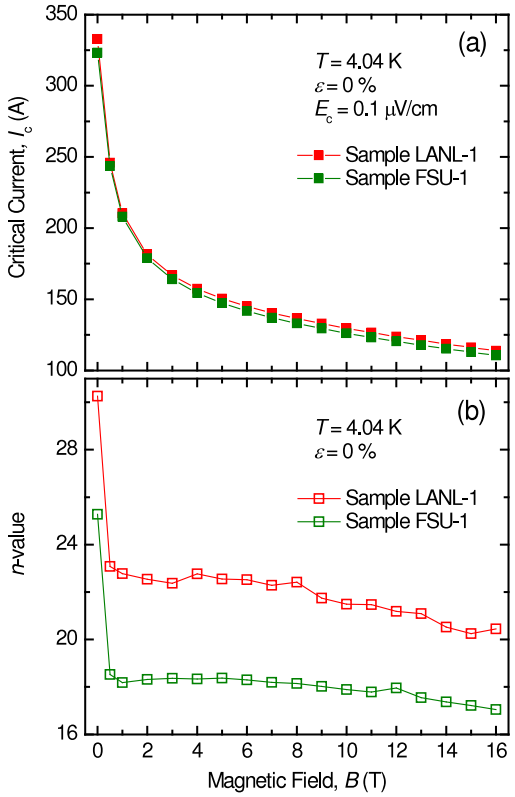


**Figure 1.** Comparisons of (a) $I_c(B)$ and (b) $n$-value($B$) in ascending $B$ from self-field to 16 T, at 4.0 K and zero applied strain, for samples LANL-1 and FSU-1. The heat-treatment schedules applied to the two samples were fairly dissimilar. Differences in $I_c(B)$ were minor nevertheless, but variations in $n$-value($B$) were more obvious.

Bi-2212 conductors [19, 27–29]. As expected, the $I_c(B)$ dependence is fairly small at high magnetic fields.

Interestingly, despite the fact that the heat-treatment schedules for the two samples were dissimilar, except for the maximum temperature, differences in their $I_c$ values were very small (figure 1(a)). LANL samples investigated herein consistently had slightly higher values of $I_c$ by ≈3% at all fields, as compared to FSU specimens. In contrast, the $n$-value showed more significant dissimilarities (figure 1(b)). Overall, it is fair to say that the performance of this wire was not very sensitive to differences in the LANL and FSU heat-treatment schedules, which may indicate that fabrication of Bi-2212 conductors has reached some degree of maturity.

For some samples, $I_c(B)$ was measured in ascending fields up to 16 T and then in descending fields to estimate the magnitude of the hysteretic behavior of $I_c(B)$. At 5 T, this hysteresis was about 6% and 8% for FSU and LANL samples, respectively. This may be another indication that the quality of the samples heat-treated at LANL and FSU was similar.

### *5.2. Critical current and n-value dependences on axial strain*

#### *5.2.1. Effect of tensile strain.*

*5.2.1a. Reversible tensile strain effect.* Figures 2(a) and (b) depict the effects of axial tensile strain on $I_c$ and $n$-value, measured at 4.0 K and 16 T, for sample LANL-1. The sample was loaded and (partially) unloaded several times to re-examine the irreversible nature of $I_c$ behavior with strain,

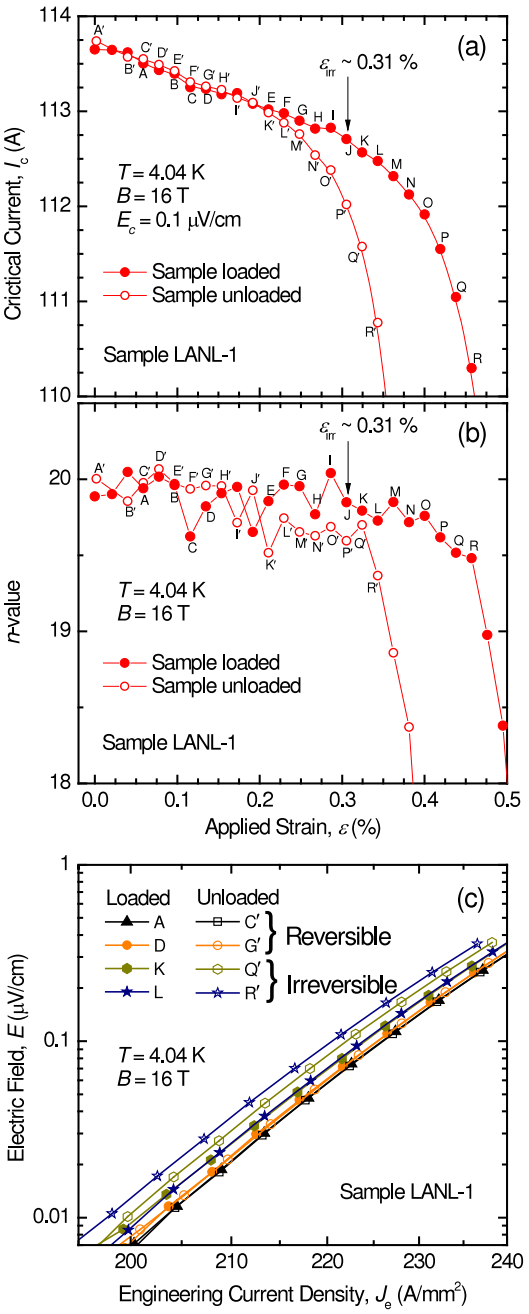


**Figure 2.** Results of (a) $I_c(\varepsilon)$, (b) $n$-value($\varepsilon$) and (c) $E$–$J$ curves for a selection of strain values, obtained in tensile strain at 4.0 K and 16 T for sample LANL-1. Each pair of unprimed and primed letters used in (a) and (b) indicates a loaded strain point (solid symbol) and its corresponding partially unloaded strain point (empty symbol), respectively. $I_c$ and $n$-value showed an unambiguous reversible behavior with strain up to at least the strain point J. $E$–$J$ curves in (c) of the loaded and unloaded points that have the same strain within the reversible regime fall on top of each other independently of the electrical-field criterion from less than 0.01 to 0.4 $\mu$V cm$^{-1}$.

**Table 1.** Summary of average $\varepsilon_{irr}$ values, where applicable, obtained for the three segments measured in each sample. Values of the slope $dI_c/d\varepsilon$ are also reported over the strain window indicated in the table for each case.

| Sample | $B$ (T) | Strain regime | Strain window (%) | Slope $dI_c/d\varepsilon$ (% per % strain) | Reversible? | $\varepsilon_{irr}$ (%) |
|---|---|---|---|---|---|---|
| LANL-1 | 16 | Tension | 0–0.29 | −2.7 | Yes | 0.32 |
| LANL-2 | 16 | ” | ” | −2.6 | Yes | 0.32 |
| FSU-1 | 16 | ” | ” | −2.9 | Yes | 0.31 |
| FSU-2 | 5 | ” | ” | −3.2 | Unclear | |
| FSU-3 | 5 | ” | Before strain cycling: 0–0.23 | −5.8 | No | |
| | | | After strain cycling: 0–0.23 | −2.4 | Yes | 0.25 |
| LANL-3 | 16 | Compression | −0.1 to 0 | −2.8 | — | |
| | | | −0.86 to −0.19 | −1.9 | — | |
| FSU-4 | 5 | Compression and tension | After cycling: −0.31 to +0.13 | −1.4 | Yes | |

discussed above. Each pair of unprimed and primed letters used in figures 2(a) and (b) indicates a loaded strain point (solid symbol) and its corresponding partially unloaded strain point (empty symbol), respectively. For example, strain was applied incrementally to point A and released at point A′, then increased to point B and released at point B′, and so on. $I_c$ and $n$-value were measured for each loaded and unloaded points to make comparisons.

Surprisingly, $I_c$ showed an unambiguous reversible behavior with strain up to at least the strain point J, whose corresponding unloaded point J′ fell on the original $I_c(\varepsilon)$ curve just as the preceding unloaded points A′ to I′ did (see figure 2(a)). It is only after strain was increased to point K that its corresponding unloaded point K′ started to deviate from the original curve. As shown in figure 2(a), the irreversible strain limit $\varepsilon_{irr}$, which is defined as the loaded strain that generated the first splitting of the loaded and unloaded $I_c(\varepsilon)$ curves due to a permanent degradation of $I_c$, is as high as 0.31%. The other two taps measured of this sample also showed reversibility up to about the same value of $\varepsilon_{irr}$. The average value of $\varepsilon_{irr}$ over the three segments measured in this sample was ≈0.32%. Within the reversible regime, $I_c$ exhibited a linear decrease with $\varepsilon$ at a slope $dI_c/d\varepsilon = \alpha \approx -2.7\%$ per percent strain (table 1). Beyond $\varepsilon_{irr}$, $I_c(\varepsilon)$ showed a nonlinear but gradual decrease with strain, followed by a precipitous drop that indicated a catastrophic failure of the sample when strain was increased further. The slope $dI_c/d\varepsilon = \beta$ that describes the steepest part of this precipitous drop varies significantly from sample to sample due to its extrinsic nature. To give an idea, we can take as a reference the average value $\beta \approx -270\%$ per percent strain that was estimated over several samples. This value is roughly 100 times steeper, as compared to the slope $\alpha$ that describes the reversible region. Please note that this comparison is indicative only, and is not intended to correlate reversible and irreversible effects.

Equally, the $n$-value showed a reversible behavior with strain (see figure2(b)). Estimations of $\varepsilon_{irr}$ from $n$-value($\varepsilon$) and $I_c(\varepsilon)$ yielded a similar result, even though the $n$-value is significantly more noisy than $I_c$.

Observation of a reversible strain effect was confirmed on the three segments of sample LANL-2, also measured at 4.0 K and 16 T. Results obtained on samples LANL-1 and LANL-2 were very analogous (see table 1).

The $E$–$J$ curves were analyzed carefully to determine whether the observed reversible behavior is effectively intrinsic to Bi-2212 or stems from current shunting through the conductive Ag matrix that surrounds Bi-2212 filaments. Figure 2(c) compares $E$–$J$ curves of the strain points A and C′, D and G′, K and Q′, and L and R′ over electrical fields ranging from less than 0.01 to about 0.4 $\mu$V cm$^{-1}$. This comparison is made between loaded and unloaded strain points that have the same strain values (refer to figure 2(a)). For example, points A and C′ have the same strain. The pairs (A, C′) and (D, G′) are within the reversible regime, and the pairs (K, Q′) and (L, R′) are outside this regime. As shown in figure 2(c), the $E$–$J$ curves of strain points A and C′ fall on top of each other, independently of the electric-field criterion. The same holds for the $E$–$J$ curves of strain points D and G′. In contrast, the $E$–$J$ curves of strain points K and Q′ are separated from each other and so is the case for the $E$–$J$ curves of strain points L and R′. Undeniably, these results not only provide evidence that a reversible strain effect can exist in Bi-2212 conductors, but also demonstrate that it can be detected at very sensitive electric-field criteria as low as 0.01 $\mu$V cm$^{-1}$. The latter evidence effectively rules out current shunting (through Ag) to be the cause of the observed reversibility of $I_c(\varepsilon)$ and $n$-value($\varepsilon$), and proves that this behavior is indeed inherent to the Bi-2212 material.

The same study was made on sample FSU-1 at 4.0 K and 16 T, and the results are presented in figure 3. $I_c(\varepsilon)$ and $n$-value($\varepsilon$) also showed a reversible behavior (figures 3(a) and (b)). The average value of $\varepsilon_{irr}$ among the three segments measured of this sample was ≈0.31%, consistent with samples LANL-1 and LANL-2. The slope $dI_c/d\varepsilon = \alpha$ within the reversible strain regime was ≈−2.9% per percent strain, also similar to that of samples LANL-1 and LANL-2 (table 1). Finally, comparisons of the $E$–$J$ curves of sample FSU-1 within the reversible regime showed that reversibility was detected over a wide range of electric-field criteria from less than 0.01 to about 0.8 $\mu$V cm$^{-1}$ (figure 3(c)).

*5.2.1b. The two-component model.* The finding of a reversible effect of strain in Bi-2212 conductor is very encouraging and boosts success prospects of high-field magnet development. It also changes some of the fundamental concepts of the descriptive model, since the latter is based entirely on irreversibility [14]. Nevertheless, it is worth mentioning that we did not observe a rigorous strain reversibility in all Bi-2212 samples investigated. Samples FSU-2 and FSU-3, both measured at 4.0 K and 5 T, at first

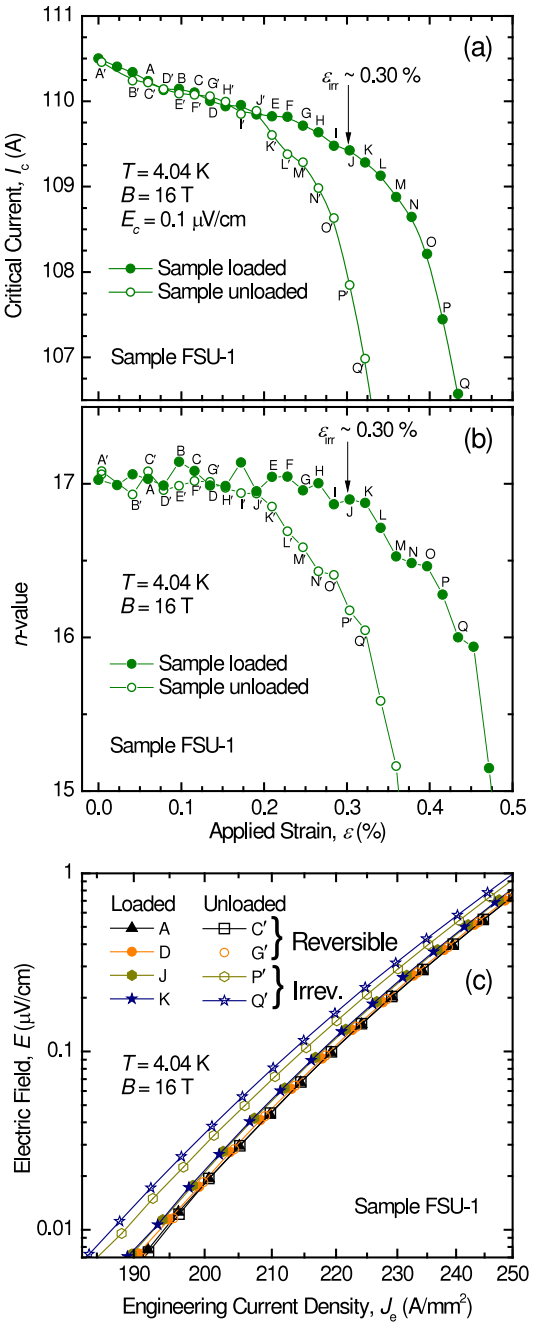


**Figure 3.** Results of (a) $I_c(\varepsilon)$, (b) $n$-value ($\varepsilon$) and (c) $E$–$J$ curves for a selection of strain values, obtained in tensile strain at 4.0 K and 16 T for sample FSU-1. Each pair of unprimed and primed letters used in (a) and (b) indicates a loaded strain point (solid symbol) and its corresponding partially unloaded strain point (empty symbol), respectively. $I_c$ and $n$-value showed an unambiguous reversible behavior with strain up to at least the strain point J. $E$–$J$ curves in (c) of the loaded and unloaded points that have the same strain within the reversible regime fall on top of each other, independently of the electrical-field criterion from less than 0.01 to 0.8 $\mu$V cm$^{-1}$.

showed irreversible behavior but became reversible after they received strain cycling. As presented in figure 4, sample FSU-2 had a very small but clear irreversible behavior (0.2% in magnitude) between zero applied strain and strain point E,

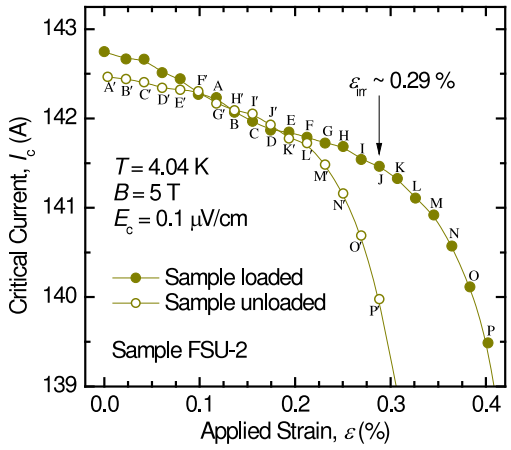


**Figure 4.** Results of $I_c(\varepsilon)$ obtained in tensile strain at 4.0 K and 5 T for sample FSU-2. There was a very small but clear irreversible behavior (0.2% in magnitude) between zero strain and strain point E. However, as strain was increased further, the sample entered into a reversible behavior between strain points F and J before reaching the failure point.

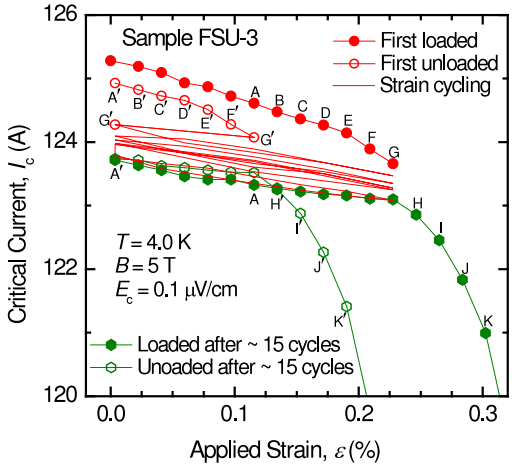


**Figure 5.** Results of $I_c(\varepsilon)$ obtained in tensile strain at 4.0 K and 5 T for sample FSU-3. There was a very small but clear irreversible behavior (0.3% in magnitude) that persisted up to the maximum applied strain of 0.23% (point G of the red curve). However, after the sample was subjected to ≈15 strain cycles between 0% and 0.23%, it started to behave reversibly (green curves) even if the strain cycling had induced ≈1.6% degradation of $I_c$ with respect to its initial value. Labeling of some of the strain points was omitted for clarity.

seeing that the unloaded points A′ to E′ fell below the original curve. However, as strain was increased further, the sample entered into a reversible behavior between strain points F and J before reaching the failure point. Sample FSU-3 also showed irreversibility with a very similar magnitude (0.3%) at first but, unlike sample FSU-2, this irreversible behavior persisted up to the maximum applied strain of 0.23% (point G of the red curve in figure 5). The interesting point, however, is that, after the sample was subjected to ≈15 strain cycles between 0% and 0.23%, it started to behave reversibly (the green curves in figure 5), even if the strain cycling had induced ≈1.6% degradation of $I_c$ with respect to its initial value.

The peculiar behavior depicted in figures 4 and 5 does not negate the possibility of a reversible effect of strain in Bi-2212 conductors. Indeed, the proof of existence of this effect was clearly established from the results presented in figures 2 and 3. What the results in figures 4 and 5 do reveal is that the sample perhaps contains two Bi-2212 components, one 'weak' and the other 'strong' mechanically. If the weak component participates in transporting current, it will induce an irreversible behavior of $I_c(\varepsilon)$ until this component breaks up mechanically through strain application or cycling, to the extent that it no longer contributes to $I_c$. Once this happens, the remaining strong component would then show reversibility of $I_c(\varepsilon)$. If the weak component does not contribute to transport current in a virgin sample due to its insufficient connectivity over significant lengths, the reversible strain effect will be manifest from the onset of the strain experiment, as was the case for samples LANL-1, LANL-2 and FSU-1. We will discuss this hypothesis (named the two-component model) in more detail in section 6, once we have presented the microstructure of the Bi-2212 samples. A similar concept of electromagnetically and mechanically weak and strong components was also suggested for Bi-2223 conductor tapes subsequent to different experimental observations [30–32].

The slope $dI_c/d\varepsilon$ $(=\alpha)$ characterizing the intrinsic $I_c(\varepsilon)$ effect in tensile strain is $\approx -2\%$ to $-3\%$ per percent strain at 4.0 K and 16 T (table 1). This value tends to increase (in absolute terms) when the $I_c(\varepsilon)$ behavior is irreversible. For example, sample FSU-3 had $\alpha \approx -5.8\%$ per percent strain before strain cycling when $I_c(\varepsilon)$ was irreversible (figure 5). After the strain cycling and the subsequent reversible behavior, this value was more than halved ($\alpha \approx -2.4\%$ per percent strain). Also, sample FSU-2, which showed small irreversibility before entering into a reversible regime, had $\alpha \approx -3.2\%$ per percent strain (table 1). Moreover, values of $\alpha \leqslant -4\%$ per percent strain were reported by ten Haken *et al* for samples that behaved irreversibly [12, 14]. Based on these observations and comparisons, we think that a characteristic value range for $\alpha$ when the $I_c(\varepsilon)$ behavior is entirely reversible is $\approx -2.5 \pm 0.5\%$ per percent strain (at 4.0 K and magnetic field from 5 to 16 T). If there is an irreversible component in the $I_c(\varepsilon)$ behavior, $\alpha$ can be doubled (in absolute terms). Hence, the value of $\alpha$ gives an indication as to whether the $I_c(\varepsilon)$ behavior is entirely reversible or not, and perhaps is commensurate with the level of contribution of the weak component to transport current. Obviously, if both reversible and irreversible components are present, probing the intrinsic effects becomes difficult and interpreting the results quite ambiguous.

*5.2.2. Effect of compressive strain.* Figure 6 describes the effect of axial compressive strain on $I_c$, measured at 4.0 K and 16 T, for sample LANL-3. The load–unload experiment was conducted for small compressive strain values down to $\approx -0.1\%$ in order to re-examine the irreversibility of $I_c(\varepsilon)$ in compression [12, 14]. This corresponds to the region highlighted by the blue rectangle in figure 6(a) and is presented in detail in figure 6(b). As expected, the behavior of $I_c(\varepsilon)$ was indeed irreversible. Thereafter, $I_c(\varepsilon)$ was measured

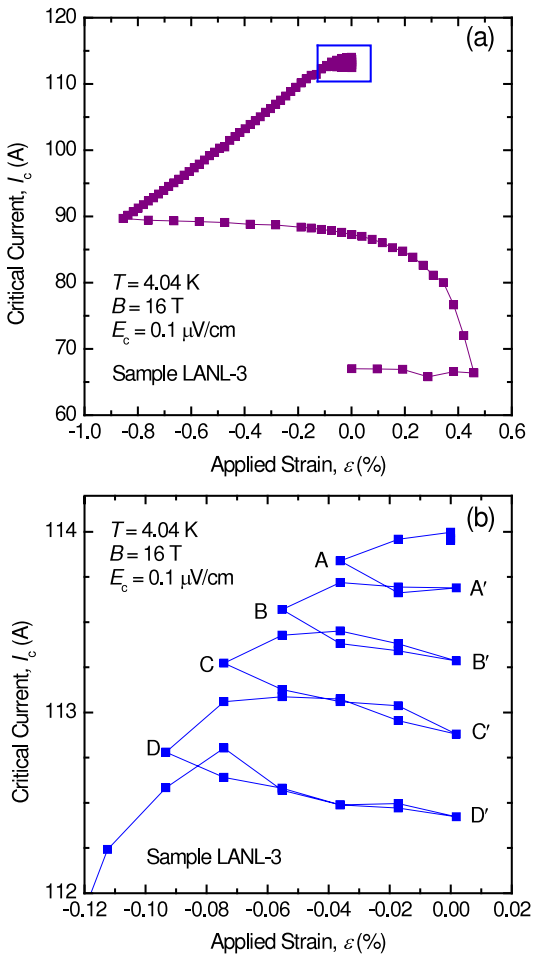


**Figure 6.** Results of $I_c(\varepsilon)$ obtained in compressive then tensile strain at 4.0 K and 16 T for sample LANL-3. (a) $I_c$ degraded fairly linearly and rapidly with compressive strain down to $-0.86\%$, where the irreversible degradation was $\approx 21\%$. Upon releasing compression and increasing strain into tension up to $+0.46\%$ and then back to zero strain, the total $I_c$ irreversible degradation was $\approx 41\%$. (b) shows details of the data highlighted by the blue rectangle in (a). The load–unload experiment revealed that the $I_c(\varepsilon)$ behavior is irreversible for any amount of compressive strain applied to the sample. Nonetheless, upon releasing compression and then applying it, $I_c(\varepsilon)$ behavior was 'reversible' as long as the reapplied compression did not go near or beyond the compressive strain reached before unloading started.

while monotonically changing compressive strain down to $\approx -0.86\%$. $I_c$ degraded fairly linearly and rapidly with $\varepsilon$ at a slope $dI_c/d\varepsilon = \gamma \approx +26\%$ per percent strain, which is roughly ten times steeper as compared to the slope $\alpha$ in the tensile reversible region (table 1), but only a tenth of the slope $\beta$ describing the steepest $I_c$ drop in tension beyond the failure point. Again, comparison between $\gamma$ and $\alpha$ is suggestive only and is not intended to correlate reversible and irreversible effects. At $\varepsilon \approx -0.86\%$, $I_c$ degraded irreversibly by $\approx 21\%$, consistent with results obtained on a different Bi-2212 wire [26]. Upon releasing compressive strain, $I_c(\varepsilon)$ followed a fairly linear behavior up to a strain $\approx -0.19\%$, with a much smaller slope $dI_c/d\varepsilon \approx -1.9\%$ per percent

strain (see figure 6(a) and table 1). This behavior has a very similar aspect to that of the samples measured under tensile strain (see figures 2(a), 3(a), 4 and 5), except that the length of the $I_c(\varepsilon)$ pseudo-plateau is at least twice as wide, which is consistent with the descriptive model [14]. As strain was released to zero and further increased into tension, $I_c(\varepsilon)$ started a nonlinear but gradual decrease until a failure point was reached where it dropped precipitously. At $\varepsilon \approx +0.46\%$, strain was released back to zero and again $I_c(\varepsilon)$ followed a pseudo-plateau, as expected by the descriptive model [14]. After this sample conditioning under compression and tension, $I_c$ degraded irreversibly by ≈41% with respect to its initial value at zero applied strain.

The precipitous drop of $I_c$ that occurred almost as soon as a compressive strain is applied to a virgin sample creates a clear discontinuity (centered around zero applied strain) in the behavior of $I_c(\varepsilon)$ as a function of tensile and compressive strains, since the slopes $\alpha$ and $\gamma$ differ by about a factor of 10 [12, 14, 26]. However, once a certain compressive strain is applied and then released, this singularity disappears [14, 26]. In lieu, $I_c(\varepsilon)$ follows a wide pseudo-plateau without a discontinuity when transiting from compression to tension, meaning that $I_c(\varepsilon)$ behavior no longer discerns between compression and tension as long as the strain stays below the failure point.

Also, it is worth noticing some fine details of the load–unload experiment presented in figure 6(b). Any small amount of compression induced an irreversible drop of $I_c(\varepsilon)$. Upon releasing compressive strain from a certain value to zero, $I_c(\varepsilon)$ decreased linearly but *increased* reversibly when compressive strain was applied again. This 'reversibility' after the initial damage persisted until compressive strain nearly matched the value it had before unloading started. For example, releasing compression from point D to D′ generated a small decrease of $I_c$, as shown in figure 6(b). However, when strain was changed back from point D′ towards D, $I_c$ increased reversibly with strain up to nearly point D. This shows that, after the irreversible damage that occurred following the application of a certain compressive strain, $I_c(\varepsilon)$ can exhibit a 'reversible' behavior as long as strain does not go near to or beyond the compressive strain value that was reached before unloading started. Interestingly, the slope $dI_c/d\varepsilon$ between points D and D′ is ≈−2.8% per percent strain, a value that is very similar to that obtained for samples measured under tensile strain within the reversible region (table 1). Similar observations of reversibility of $I_c(\varepsilon)$ in compression after the initial damage were also made recently in Bi-2223 conductor tapes at both temperatures, 4.2 and 77 K [33].

To further investigate this subtle point, 'reversibility' (after the initial damage) was examined in sample FSU-4 in compressive and tensile regimes combined. This specimen was measured in compression down to −0.31%. $I_c(\varepsilon)$ was irreversible, as expected. Subsequently the sample was subjected to strain cycling about 35 times between −0.31% and 0%. Once $I_c(\varepsilon)$ seemed fairly stable with strain cycling, a load–unload experiment was conducted from compression starting at −0.31% into tension up to the failure point. As presented in figure 7, after such strain cycling, $I_c$ showed a

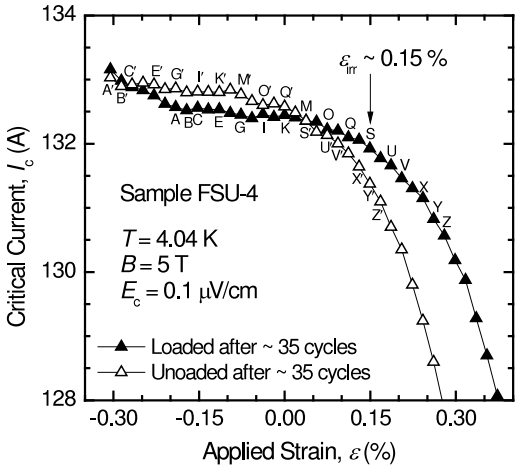


**Figure 7.** Results of the load–unload experiment obtained in both the compressive and tensile strain regimes at 4.0 K and 5 T for sample FSU-4. This specimen was measured in compression down to −0.31%, and then was subjected to ≈35 strain cycles between −0.31% and 0% until $I_c(\varepsilon)$ seemed fairly stable with cycling. After strain cycling, $I_c(\varepsilon)$ showed a reversible behavior (unloaded points are, in fact, slightly above the loaded curve) both in compression and in tension up to $\varepsilon_{irr} \approx +0.15\%$, but the reversible pseudo-plateau extended over a strain window of ≈0.46%, which is significantly wider than the 0.3% that was measured when only tension was applied, and was shifted towards compressive strains. Labeling of some of the strain points was omitted for clarity.

reversible behavior with strain (unloaded points are actually even slightly above the loaded curve) both in compressive and tensile regions up to $\varepsilon_{irr} \approx +0.15\%$. More importantly, the reversible pseudo-plateau extended over a strain window of ≈0.46%, which is significantly wider than the 0.3% that was measured when only tension was applied (samples LANL-1, LANL-2 and FSU-1), although this pseudo-plateau had shifted towards compressive strains. Furthermore, within this reversible plateau, $I_c(\varepsilon)$ had a fairly linear behavior without a discontinuity when going from compression to tension. The slope $dI_c/d\varepsilon$ over both the compressive and tensile regimes was estimated as ≈−1.4% per percent strain.

Based on these results, we postulate that, in the case of a virgin Bi-2212 sample, if compression did not induce the irreversible (extrinsic) damage such as that shown in figure 6, $I_c$ might have exhibited the same linear and reversible behavior under compression as in tension until a certain irreversible compressive strain limit $\varepsilon_{irr}$ is reached. In other words, the intrinsic response of Bi-2212 material to compressive strain would probably be a reversible increase of $I_c$ following a similar slope $dI_c/d\varepsilon$ ($=\alpha$) as in tension without a discontinuity at zero applied strain. However, due to some extrinsic factors relating to the conductor's microstructure, we end up seeing a precipitous and irreversible decrease of $I_c$ when a compressive strain is applied to the sample. If this postulate is correct, it would have interesting ramifications for magnet applications. We will discuss this postulate and the proposed modified descriptive strain model in more detail in sections 6 and 7 once we have identified the possible origin of irreversibility in compression.

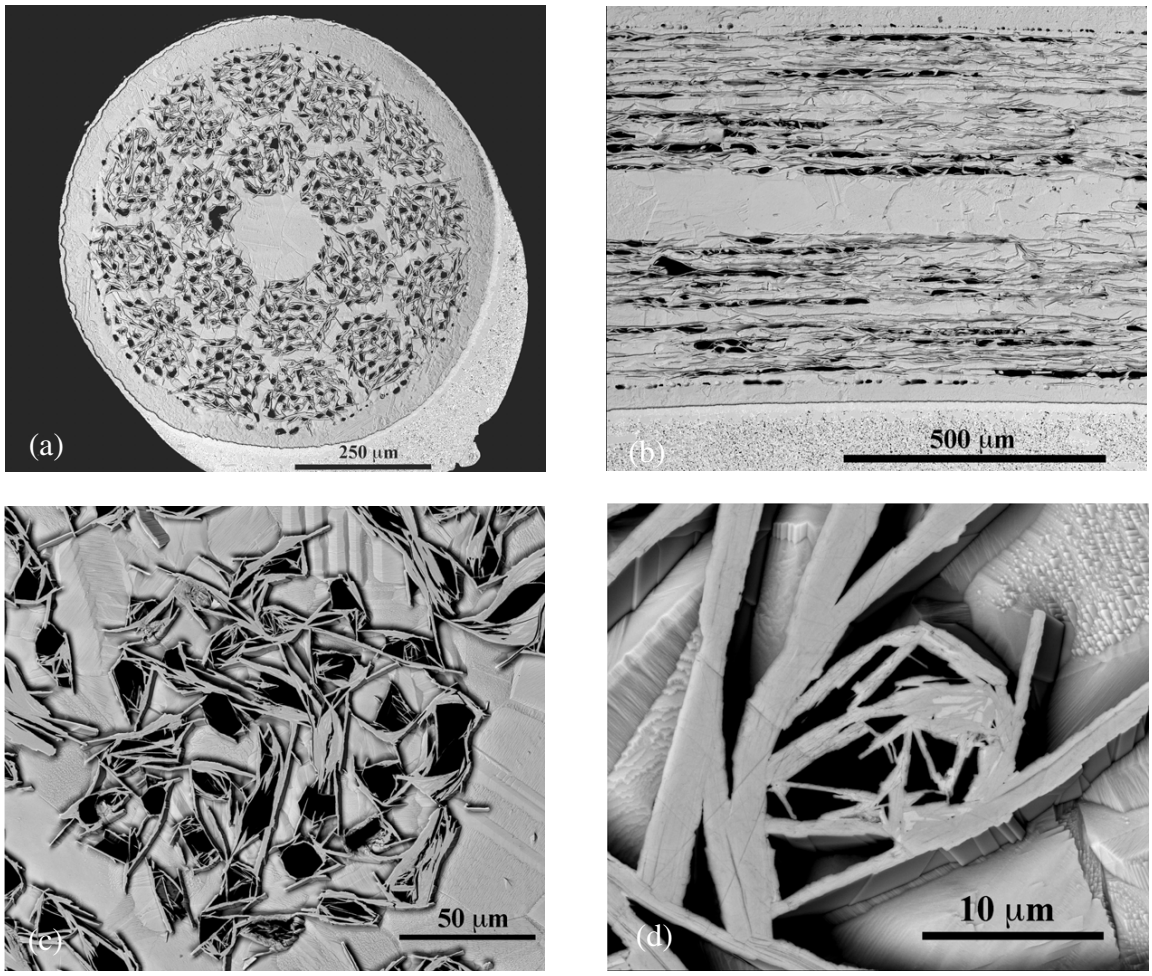


**Figure 8.** SEM micrographs showing the microstructure of sample FSU-2 after measurements in tension. (a) presents a sample's transverse cross section showing the 18 sub-elements of the wire. A layer of Pb–Sn solder used for mounting the sample onto the Walters' spring can be seen on the outside of the sample. (b) depicts a longitudinal cross section where four sub-elements across the wire diameter are visible. Growth of Bi-2212 through the Ag matrix caused filaments to interconnect via bridges in such a way that the filaments were no longer easily discernible from each other after the heat treatment. (c) shows one sub-element containing 37 filaments intertwined with each other in a complex pattern. (d) zooms into one of these filaments. All these figures clearly show significant Bi-2212 outgrowth and high porosity in the wire. The overwhelming majority of filaments have pores that extend longitudinally over significant lengths.

## 6. Microstructure and its relation to the strain effect

Microstructure of the Bi-2212 conductor is key to understanding the effect of strain in this material, and will help us substantiate the two-component model proposed in section 5.2.1b as well as the modified descriptive strain model to be described in section 7.

Figures 8(a)–(d) give an overview of the wire microstructure. Although these SEM pictures were taken on sample FSU-2, they actually represent the main microstructural features seen in all the specimens investigated. Figure 8(a) presents a sample's transverse cross section showing the 18 sub-elements and figure 8(b) is for a longitudinal cross section where four sub-elements across the wire diameter are visible. Growth of Bi-2212 through the Ag matrix had caused filaments to interconnect via bridges in such a way that the filaments were no longer easily discernible from each other after the heat treatment. Figure 8(c) shows one sub-element containing 37 filaments intertwined with each other in a complex pattern, and figure 8(d) zooms into one of these filaments. All these figures clearly show high porosity in the wire. The overwhelming majority of filaments have pores (figure 8(a)) that extend longitudinally along the wire axis over significant lengths (figure 8(b)). Note that these pores were purposely filled with epoxy during the specimens' preparation for SEM investigation, assuring us that porosity was not the result of material pullout during the polishing process.

The Bi-2212 outgrowth and porosity features have been known for some time [22, 27, 34–38]. Regarding porosity in particular, its omnipresence in the Bi-2212 microstructure has been revealed clearly [35–38]. Pores can stretch over most of the width of a filament at various locations in a multifilamentary wire and, as a result, seriously impede the flow of transport current through the wire length [38].

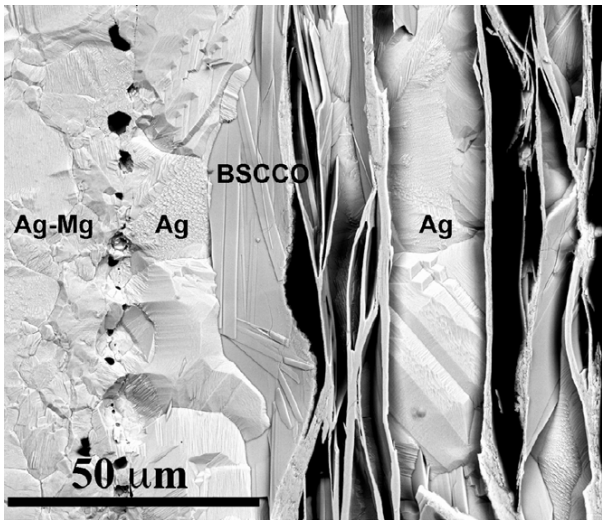


**Figure 9.** SEM micrograph showing a longitudinal cross section of sample LANL-4 after measurements in tension. The heat treatment formed dense Bi-2212 grain colonies at the interface with the Ag matrix. On the other hand, a fibrous network of Bi-2212 grains formed inside the filament. The two-component model postulates that the dense Bi-2212 is the strong component and that the porous and fibrous Bi-2212 network is the weak component. Defects can be seen at the interface between the outer Ag–Mg sheath and Ag matrix, which probably formed during the wire fabrication.

Interconnections between filaments via Bi-2212 outgrowths (bridges) probably provide alternative paths for current to circumvent some of the obstacles created by pores. Just as the microstructural studies showed the seriousness of the porosity factor in the Bi-2212 conductor [35–38], they also revealed the significant margin for progression that is still available to improving $J_c$ in this conductor if porosity can be overcome. The present work will show that porosity has far-reaching ramifications in that it also weakens the tolerance of the Bi-2212 conductor to mechanical strain.

In section 5.2.1b, we proposed the two-component model to interpret the results presented in figures 4 and 5. We suspected that the lack of a clear reversibility of $I_c(\varepsilon)$ in samples FSU-2 and FSU-3 may be due to the presence in the conductor of mechanically strong and weak Bi-2212 components. Figures 8(d) and 9 show that a dense colony of Bi-2212 grains had formed at the interface between the filament and the Ag matrix and that, on the other hand, a fibrous network of Bi-2212 grains had occupied the inside of the filament. This is consistent with the shell model developed by Holesinger *et al* to describe the microstructure of Bi-2223 multifilamentary tapes [39]. We postulate that the dense Bi-2212 that formed adjacent to Ag is the strong component, and that the one that developed away from the interface with Ag is the weak component. The latter component has significant porosity within and around it, and hence seems mechanically not well supported. As a result, this component is more prone to cracking under strain, as compared to the strong component. Hence, if the weak component contributes to $I_c$, it will cause irreversibility of $I_c(\varepsilon)$. This irreversible behavior will disappear eventually once this component's connectivity (current path) is broken through increasing or cycling strain. If, however, this weak component does not contribute to $I_c$ in a virgin sample, its cracking under strain will not be detected by transport measurements, and reversibility of $I_c(\varepsilon)$ will be observed (see figures 2 and 3). High magnetic field and/or temperature could potentially interrupt the connectivity of the weak component if this connectivity is established at some locations via superconducting weak links. This might be the reason why we saw reversibility at 16 T, but not so clearly at 5 T. We do not necessarily assume that the two components have different compositions. Rather, we suggest that the brittleness of the weak component stems primarily from the lack of structural support around it, and hence is a direct consequence of the presence of porosity in the wire. However,

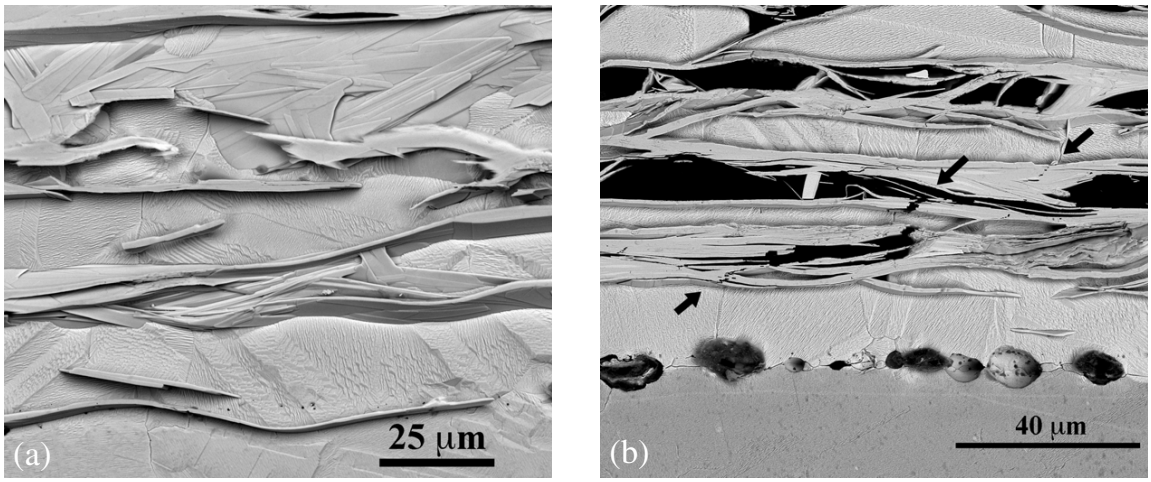


**Figure 10.** SEM micrographs showing longitudinal cross sections of sample FSU-2 after measurements in tension. (a) depicts a section of the sample with dense Bi-2212 filaments. (b) presents a section of the sample with high porosity. The dense region showed no apparent cracks, whereas the porous region had several cracks (highlighted by the arrows) that cut severely through the Bi-2212 filaments. This substantiates the possibility of a close correlation between porosity and crack formation.

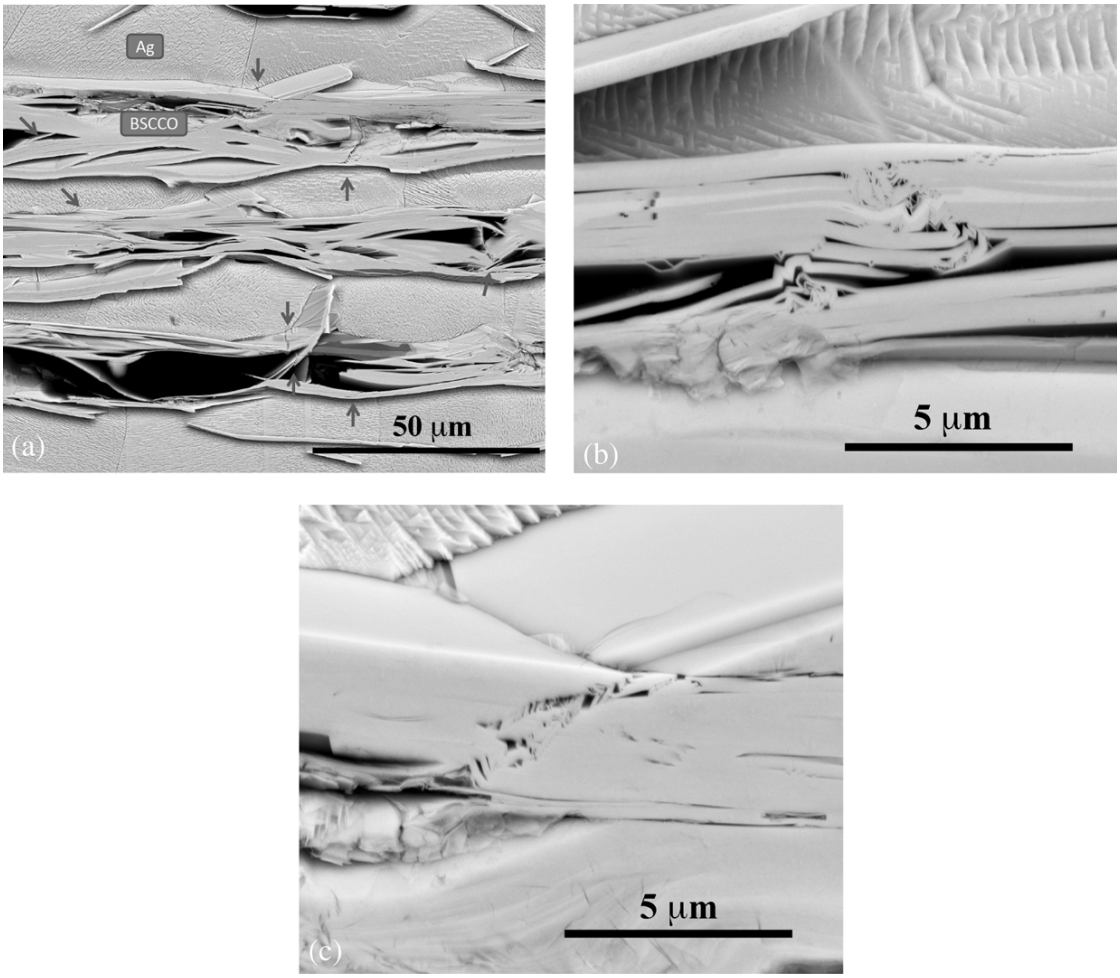


**Figure 11.** SEM micrographs showing longitudinal cross sections of sample LANL-3 after measurements in compression and then in tension. (a) depicts several buckling defects (highlighted by the arrows) in Bi-2212 filaments. (b), (c) show some of these buckling defects in greater detail. These defects are close to porosity, and can cause Bi-2212 grain colonies to separate (delaminate) from each other. The buckling defects are believed to be due to compressive axial strain only, and that they are the primary cause for the irreversible behavior of $I_c(\varepsilon)$ under compressive strain in Bi-2212 wires.

we do not exclude that secondary phases in the filament core could potentially contribute to the brittleness of the weak component.

Other evidence of the detrimental effect of porosity is shown in figure 10 for sample FSU-2. This sample was measured in tension up to ≈0.53% before imaging. The figure contrasts a region in the sample containing no porosity (figure 10(a)) with another region that has a significant amount of porosity (figure 10(b)). The dense region showed no apparent cracks, whereas the porous region had several cracks that cut severely through the Bi-2212 filaments. This substantiates the possibility of a close correlation between porosity and crack formation. Evidently, even dense regions will eventually crack when strain is increased beyond a certain level, but the contrasting images in figure 10 hint that the wire's failure point in tension could be pushed to strains higher than ≈0.4% if porosity could be eliminated.

We have shown that the irreversible degradation of $I_c(\varepsilon)$ under compressive strain happens at a rate that is about a tenth of that under tensile strain beyond the failure point ($\beta \approx -10\times\gamma$). This suggests that the failure mode in compression is probably of a nature different from that in tension. Indeed, the longitudinal cross section in figure 11 reveals buckling of Bi-2212 grains in sample LANL-3 measured under compressive strain. This kind of defect was seen neither in samples measured only in tension nor in unstrained samples. Even though sample LANL-3 was measured in compression down to −0.86% and then taken into tension up to +0.46%, we think that the grain buckling was due only to axial compression.

The buckling of grains was accompanied by a separation (delamination) of some colonies of Bi-2212 grains from each other (figures 11(b) and (c)). Notice that buckling occurred in the strong component (adjacent to Ag) as well as in the weak component. This explains why reversibility was not present in the virgin samples subjected to axial compression, since neither of the two components were intact all the way through the current path. Notice also that, where buckling occurred, porosity was not far from its vicinity (figure 11). Here also,

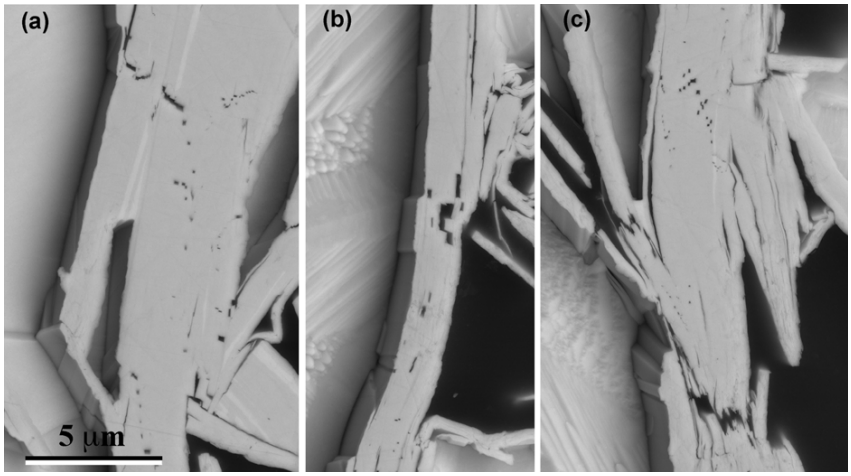


**Figure 12.** SEM micrographs showing transverse cross sections of sample LANL-3 after measurements in compression and then in tension. Defects visible in (a) and (b) could possibly have been formed under the effect of compressive axial strain, but some of those shown in (c) could have been the result of the subsequent tensile axial strain.

porosity probably plays an important role in promoting grain buckling in compression due to the lack of structural support of the Bi-2212 grain colonies that are near it. We also think that the soft Ag matrix may not be providing much mechanical support to the grains under compression, and hence may also be contributing to grain buckling. Whereas the mechanical weakness of Ag did not prevent elastic deformation of the strong component in tension (up to $\varepsilon_{irr}$), Ag did not provide the mechanical support needed to transmit compression to Bi-2212 grains without buckling.

The transverse cross section of sample LANL-3 in figure 12 shows additional cracks and defects in the Bi-2212 component. Because this sample was measured in both compression and tension, we cannot confirm that all the cracks visible in figure 12(c) are due to compression. However, defects visible in figures 12(a) and (b) could have been possibly formed under the effect of compression.

We suggest that buckling of the grain colonies is the primary failure mode in Bi-2212 conductor under compressive strain, and the reason why a reversible strain effect was never observed (in compression) in this conductor to date [12, 14, 26]. The intrinsic response of Bi-2212 to compression, which we postulate in the modified descriptive strain model to be a linear increase of $I_c(\varepsilon)$, is veiled by the buckling of the Bi-2212 grains that instead yields a precipitous drop of $I_c(\varepsilon)$. However, once a certain compressive strain is applied and the resulting buckling damage has taken place in the sample, a reversible behavior of $I_c(\varepsilon)$ is possible when compression is reduced, as seen in figures 6 and 7. If more compression is applied, it will result in more buckling and a further decrease of $I_c$ (figure 6(b)).

## 7. The modified descriptive strain model

The descriptive model developed by ten Haken *et al* was intended to give an overview of the axial strain effects on $I_c$ in Bi-2212 conductor [14]. As we discussed in section 2, all previous strain studies converged on the irreversible and extrinsic nature of the strain effects in Bi-2212 material [10–14]. The descriptive model was proposed to portray this irreversibility, which itself is the main foundation of the model.

The descriptive model discerned three regions in the $I_c(\varepsilon)$ behavior: (a) a compressive regime where $I_c$ decreases linearly with applied compression, typically at a slope $dI_c/d\varepsilon \approx +30\%$ per percent strain; (b) a first tensile regime where $I_c$ decreases linearly with applied tension at a slope $dI_c/d\varepsilon \approx -4\%$ per percent strain; and (c) a second tensile regime where $I_c(\varepsilon)$ drops at a steep slope $dI_c/d\varepsilon$ varying between 100% and 500% per percent strain, depending on the sample. This distinction in the $I_c(\varepsilon)$ behavior pins down two discontinuities: the one at zero applied strain between the compressive and the first tensile regimes, and the other at the strain delimiting the first and second tensile regimes (approximately where $I_c$ degrades by ≈2%). The descriptive model postulates that strain at the second discontinuity equals the thermal strain that is applied to Bi-2212 during cool-down. Once applied strain compensates for the pre-compressive strain, $I_c$ starts to drop precipitously with strain. The model also postulates that $I_c(\varepsilon)$ dependences in the compressive and second tensile regimes can be extrapolated into the first tensile regime to project an $I_c$ value, where the two extrapolations intersect, attributed hypothetically to strain-free Bi-2212 not surrounded by a matrix (i.e. not inside a conductor or deposited on a substrate; see figure 2 in [14]). This extrapolated value is well above the pseudo-plateau of the first tensile regime, which means that the optimum $I_c$ value can never be obtained in a wire even when Bi-2212 reaches a strain-free state (near the second discontinuity). The model relates the difference between the $I_c$ theoretical and measured values for the strain-free state of Bi-2212 to the pre-compressive strain exerted on Bi-2212 by its surrounding matrix in a wire, and to the irreversible nature of the strain effects in this material. In other

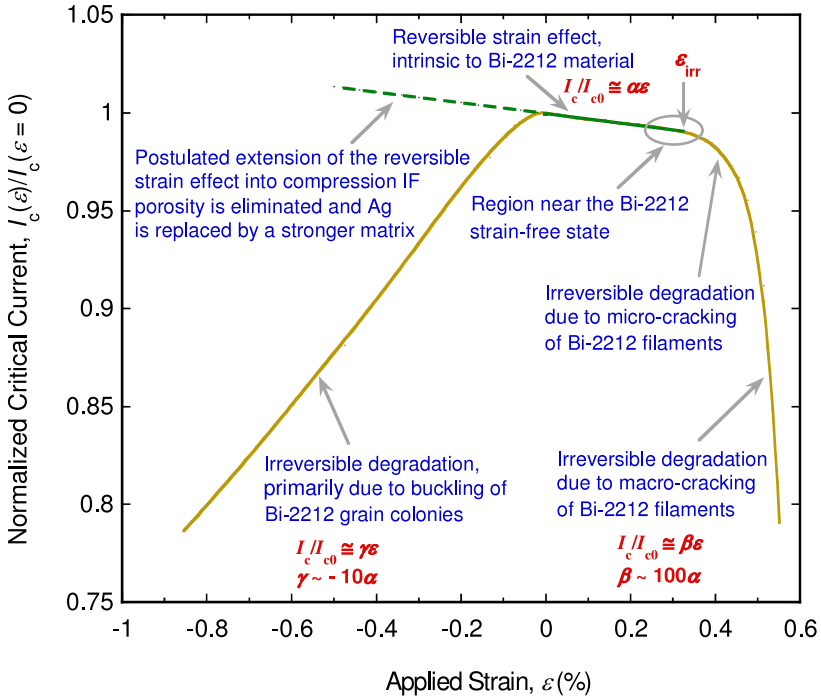


**Figure 13.** Illustration of the dependence of $I_c$ on axial compressive and tensile strains in Bi-2212 conductor according to the modified descriptive strain model. Within the first tensile regime, the value of the slope $dI_c/d\varepsilon = \alpha \approx -2.5 \pm 0.5\%$ per percent strain at 4 K and magnetic fields from 5 up to 16 T if the weak Bi-2212 component (postulated in the two-component model) does not contribute to $I_c$. If this component carries some current, the behavior of $I_c(\varepsilon)$ becomes irreversible and the slope $\alpha$ is more pronounced ($\leqslant -4\%$ per percent strain). The relations of the slopes $\alpha$, $\beta$ and $\gamma$ are indicative only, and are not intended to correlate reversible and irreversible effects. Values of $\beta$ and $\gamma$ are probably linked to the amount of porosity in the wire. The new model postulates that, if buckling of Bi-2212 grains could be prevented, a reversible strain effect should exist in the applied compressive regime and should give rise to an extension of the linear and reversible behavior of $I_c(\varepsilon)$ in the applied tensile regime without a discontinuity at zero applied strain.

words, the pre-compressive strain depresses $I_c$, and the higher the pre-compression, the lower $I_c$ becomes.

Our finding of a reversible strain effect in the Bi-2212 conductor brings a new element that conflicts with some of the perceptions of the descriptive model. Just the fact that reversibility exists (in tension) renders some features of the descriptive model obsolete. We clearly showed that, within the first tensile regime, $I_c$ can, in fact, intrinsically increase from its value near the strain-free state of Bi-2212 in the wire (somewhere near $\varepsilon_{irr}$) when applied strain is decreased (see unloaded points in figures 2(a) and 3(a)). This should simulate the effect of applying pre-compression to Bi-2212, and implies that pre-compression should actually increase $I_c$, not decrease it. This conclusion is in sharp contradiction with the descriptive model postulate that $I_c$ should decrease with pre-compression from its projected value above the pseudo-plateau at the Bi-2212 strain-free state. These observations led us to develop a new model that modifies several aspects of the existing one to describe the effect of strain in the Bi-2212 conductor more accurately, as depicted in figure 13.

The new model, named the modified descriptive strain model, makes the following observations and postulates.

(1) The behavior of $I_c(\varepsilon)$ within the first tensile regime is reversible and linear up to $\varepsilon_{irr}$, with a slope $dI_c/d\varepsilon = \alpha \approx -2.5 \pm 0.5\%$ per percent strain at 4 K and magnetic fields from 5 up to 16 T if the weak Bi-2212 component (postulated in the two-component model) does not contribute to $I_c$. If, however, this component carries some current, the behavior of $I_c(\varepsilon)$ becomes irreversible and the slope $\alpha$ becomes more pronounced ($\leqslant -4\%$ per percent strain).

(2) As the descriptive model suggests, the Bi-2212 strain-free state could well be at the second discontinuity (i.e. somewhere near $\varepsilon_{irr}$). However, we think that the theoretical value of $I_c$ of Bi-2212 not inside a conductor is not above, but conceivably on, the pseudo-plateau. In other words, $I_c$ at the strain-free state of Bi-2212 in the wire is essentially the same as for Bi-2212 not surrounded by a matrix or deposited on a substrate (if abstraction is made of any differences in pinning strength between the two systems). This value is not the highest, because intrinsic compression ($0 \leqslant \varepsilon < \varepsilon_{irr}$) increases $I_c$. This implies that thermal pre-compression does not depress $I_c$ in a wire. Rather, higher thermal pre-compressive strains should improve $I_c$ if buckling of Bi-2212 grains does not occur, and should result in a wider $I_c(\varepsilon)$ pseudo-plateau in the applied tensile regime without degradation of the initial $I_c$.

(3) The three strain regimes identified by the descriptive model are valid. However, there is a fourth regime

that can be distinguished between the first tensile and second tensile regimes. In this region, $I_c(\varepsilon)$ behavior is rather parabolic. This somewhat gradual but irreversible degradation of $I_c$ is probably due to the formation of micro-cracks in Bi-2212 filaments. The description of this fourth regime is qualitative only. It is difficult to quantify its width and strain where it transits to the second tensile regime. The latter two quantities could change (increase) rapidly with (reduced) porosity in the wire.

(4) Beyond this 'additional' regime, $I_c$ degrades precipitously and mostly linearly at a slope $dI_c/d\varepsilon = \beta \approx -150\%$ to $-300\%$ per percent strain. $\beta$ is roughly $100 \times \alpha$. The degradation of $I_c$ in this regime is probably due to the formation of macro-cracks in Bi-2212 filaments, as shown in figure 10(b).

(5) The (first) discontinuity between the first tensile and compressive regimes is due primarily to the buckling of Bi-2212 grain colonies under applied compression, promoted by porosity in the Bi-2212 filaments and by the weak mechanical properties of the Ag matrix.

(6) The $I_c(\varepsilon)$ behavior in compression of the current Bi-2212 wires is a pronounced and irreversible, mostly linear, decrease of $I_c$ at a slope $dI_c/d\varepsilon = \gamma \approx +25\%$ to $+40\%$ per percent strain. $\gamma$ is roughly $10 \times \alpha$ [14] but could vary, depending on the amount of porosity in the wire. The transition between the first tensile and compressive regimes (at the first discontinuity) is abrupt enough that any intermediate regime between the two can be neglected.

(7) The intrinsic response of $I_c$ to an applied compressive strain might actually be an extension of the linear and reversible behavior of $I_c(\varepsilon)$ in the first tensile regime. This linear behavior with applied compression might be found if Bi-2212 buckling could be avoided through densification of Bi-2212 in the filaments as well as through implementation of a stronger mechanical reinforcement around the Bi-2212 filaments. If this postulate proves to be true, it would mean that $I_c$ can be actually enhanced with applied compressive strain. This would be extremely beneficial for magnet applications, since the large $I_c$ degradation in compression seen in the current Bi-2212 wires would be avoided. If porosity is reduced but not totally eliminated, and reinforcement around Bi-2212 filaments is still inadequate, we anticipate that irreversibility of $I_c(\varepsilon)$ in compression would continue to persist but that the slope $\gamma$ would be significantly reduced.

## 8. Discussion

The finding of a reversible strain effect in Bi-2212 complements the findings of this effect in RE–Ba–Cu–O [40–45] and Bi-2223 [17, 18] technological conductors. It shows that reversibility of the effect of strain on $I_c$ is more common in high-temperature superconducting (HTS) wires and tapes than originally thought from early studies. The steady improvement of the quality of HTS conductors has allowed us to probe their intrinsic properties more easily.

So far, the intrinsic strain effect in Bi-2212 is evident only under applied tensile strain, and not yet observed under applied compressive strain (except after strain cycling), unlike in RE–Ba–Cu–O-coated conductors [45] or, to a small extent, in Bi-2223 tapes [46]. We anticipate its potential existence in Bi-2212 wires under compression, but finding it would require substantial improvement of the quality of the current strands. If this postulate comes to fruition, it could open up other magnet design options, such as the cable-in-conduit conductor (CICC) technology needed for hybrid ultra-high-field magnets, tokamak reactors for magnetic fusion energy production, and superconducting magnetic energy-storage devices (SMES). Until this improvement happens, the lack of reversibility under compressive axial strain will continue to yield irreversible damage to $I_c$ from bending strain [13, 47] even if reversibility exists under tensile axial strain.

Of significance, the low yield strain ($\varepsilon_p$) of the pure Ag matrix that is $\leqslant 0.02\%$ [26] did not cause early cracking of Bi-2212 in tension, since we observed the reversible strain effect up to $\approx 0.3\%$. This may be proof that Bi-2212 is effectively under compression in a virgin sample after cool-down. This kind of disconnection between $\varepsilon_{irr}$ of the superconductor and $\varepsilon_p$ of the matrix immediately surrounding it (i.e. $\varepsilon_{irr} \gg \varepsilon_p$) was also reported in Y–Ba–Cu–O-coated conductors [40]. However, the low yield point of Ag under applied compressive strain perhaps renders Bi-2212 structurally not well supported, and thus plays a role in masking reversibility in the Bi-2212 conductor in the compressive regime. Undeniably, the wire has an Ag–Mg outer sheath that is much stronger than Ag, but it is Ag that is in immediate contact with Bi-2212 and is the predominant matrix material inside the wire. We maintain that porosity is the primary factor facilitating buckling of the Bi-2212 grain colonies in compression, but the soft Ag matrix perhaps does not provide enough structural reinforcement to Bi-2212 to adequately transmit the applied compression to it and, consequently, may also promote buckling. Replacing at least part of the Ag with a stronger and compatible alloy to provide a distributed reinforcement across the wire section would perhaps not only contribute to remediate the buckling problem, but would also improve the relatively low yield strength and possibly the Young's modulus of the current Bi-2212 wires [26]. More research for developing such strong and compatible Ag alloys is still needed [26].

The elastic deformation of Bi-2212 grains observed by ten Haken *et al* in a conductor tape [15] explains the origin of the intrinsic strain effect on $I_c$ in tension reported herein. This lattice deformation is expected to change the superconducting critical temperature ($T_c$). Indeed, it has been known for some time that $T_c$ can be reduced by applying uniaxial stress along the crystallographic axis $a$ or $b$ of the Bi-2212 lattice, and increased by applying stress along its $c$ axis [48–50]. Non-hydrostatic elastic strains applied to a Bi-2212 lattice do change the spacing between the Cu–O planes and the atomic distance between Cu and O within the Cu–O planes, and this should lead to changes in $T_c$ [50]. As in the majority of superconductor materials, variations of $T_c$ from the application of non-hydrostatic elastic strain lead to intrinsic effects of strain on $I_c$ [46, 51–54], and Bi-2212 material should be no exception.

The intrinsic effect of strain on $I_c$ in Bi-2212 is relatively small (in the first tensile regime) at 4 K in magnetic fields up to at least 16 T. For magnet design, this property should represent a major simplification over other superconducting materials, such as $Nb_3Sn$ strands for example, where the intrinsic strain effect is significantly more pronounced [51, 55]. Although the exact $T_c(\varepsilon)$ dependence in the Bi-2212 conductor is not yet known, one can reasonably expect the sensitivity of $I_c$ to strain to increase at temperatures closer to $T_c$. The slope $\alpha$ at 4 K was very similar at 5 and 16 T, probably due to the fact that temperature was far below $T_c$ (reduced temperature $t = T/T_c \ll 1$) and $B$ was also far below the effective upper critical field ($B^*_{c2}$) where the pinning force density goes to zero at 4 K (reduced field $b = B/B^*_{c2} \ll 1$). However, we expect a more pronounced dependence of $\alpha$ on magnetic field at elevated temperatures [46]. This should matter, to some extent, when designing cryo-cooled magnets to operate at elevated temperatures (around 20 K, for example), but would not be relevant to magnets operating at temperatures around 4 K.

The reversible strain effect in the Bi-2212 conductor is very useful for the development of high-field magnets. Nevertheless, unless the porosity problem is resolved, this effect will not always be present. Recent work by Jiang *et al* revealed that porosity can be reduced dramatically by use of cold isostatic pressing (CIP) or swaging of the wire prior to the heat treatment [56, 57]. Both techniques resulted in an increase of $I_c$ by a factor of two. These are very promising results, and the two methods may hopefully yield an improvement of the Bi-2212 conductor's strain properties.

We have shown how limited strain cycling can help reveal the reversible strain effect when it was not manifest in a virgin sample. However, it is not clear yet how extended fatigue cycling would influence this effect in Bi-2212 wires, especially if defects—such as delamination of grain colonies shown in figures 11(b) and (c)—are generated in the strong component through cycling. It is true that a large number of strain cycles seem to yield a saturation of the $I_c$ degradation with strain in the Bi-2223 conductor tapes [16], but this behavior remains to be investigated in Bi-2212 strands. Statistical studies are required to gain a deeper understanding of the electromechanical properties of Bi-2212 conductors [58].

## 9. Conclusion

We reported an extensive study of the effect of axial strain in a newly developed Bi-2212 round wire and its relation to the conductor microstructure. We found a reversible strain effect on $I_c$ in the tensile regime in this material. Despite the fact that this intrinsic effect was not present in all samples and did not manifest under axial compressive strain (except after strain cycling), it is very useful for magnet development and will open new opportunities for in-depth studies of the intrinsic strain properties of Bi-2212 for a better understanding of this material. This investigation identified the major role that porosity plays in limiting the resilience of the Bi-2212 conductor to strain, and anticipated that improved mechanical properties would result from eliminating it. Replacing at least part of the Ag with a stronger and compatible alloy to provide a distributed reinforcement across the wire section would also be beneficial if detrimental consequences on $I_c$ from such substitution could be avoided.

A two-component model was proposed that suggests the presence of mechanically weak and strong Bi-2212 components within the filaments. The model identifies the weak component to be the fibrous network of Bi-2212 grain colonies that generally run in the middle section of a filament, and the strong component to be the dense grain colonies adjacent to the Ag matrix. The fragility of the weak component is attributed to the porosity embedded in it, which renders this component structurally unsupported. This component does not contribute significantly to $I_c$ but, when it does so by even small amounts, it induces an irreversible behavior of $I_c(\varepsilon)$ under tensile axial strain.

The very fact that reversibility can exist in Bi-2212 conductors makes the descriptive model somewhat obsolete, since irreversibility was its foundation. We proposed a modified descriptive strain model, which introduces several revisions to the existing one. In particular, this model suggests that $I_c$ improves with the pre-compressive strain so long as buckling of Bi-2212 grains does not occur during sample cool-down. This point is in sharp contrast with the descriptive model, and suggests placing Bi-2212 under more pre-compression by incorporating appropriate Ag alloys in the wire structure. This should result in a wider plateau of $I_c(\varepsilon)$ in the applied tensile regime, without degradation of the initial $I_c$. The modified descriptive strain model identifies the main factor for $I_c(\varepsilon)$ irreversibility under applied compressive strain to be the buckling of Bi-2212 grains. This buckling arises from porosity and the lack of adequate mechanical support of Bi-2212 by the soft Ag matrix surrounding it. The new model postulates that, if buckling of Bi-2212 grains could be prevented, a reversible strain effect should exist in the applied compressive regime and should give rise to an extension of the linear and reversible behavior of $I_c(\varepsilon)$ in the applied tensile regime without a discontinuity at zero applied strain. The ramifications of such potential behavior would be significant for magnet development.

## Acknowledgments

We thank our colleagues at Los Alamos National Lab, Lawrence Berkeley National Lab, Fermi National Lab, Brookhaven National Lab, Florida State University, North Carolina State University and Texas A&M University, who are part of the Very High Field Superconducting Magnet Collaboration (VHFSMC), for many and interesting discussions. This work was supported in part by the American Recovery and Reinvestment Act through the US Department of Energy, Office of High Energy Physics. Certain commercial equipment or materials mentioned in this paper may be indirectly identified by their particular properties. Such identification does not imply recommendation or endorsement by NIST, nor does it imply that the equipment or materials identified are necessarily the best available for the purpose.

## References

[1] Weijers H W *et al* 2010 *IEEE Trans. Appl. Supercond.* **20** 576–82

[2] Hazelton D W, Selvamanickam V, Duval J M, Larbalestier D C, Markiewicz W D, Weijers H W and Holtz R 2009 *IEEE Trans. Appl. Supercond.* **19** 2218–22

[3] Markiewicz W D, Miller J R, Schwartz J, Trociewitz U P and Weijers H W 2006 *IEEE Trans. Appl. Supercond.* **16** 1523–6

[4] Weijers H W, Trociewitz U P, Marken K, Meinesz M, Miao H and Schwartz J 2004 *Supercond. Sci. Technol.* **17** 636–44

[5] Godeke A, Cheng D, Dietderich D R, Ferracin P, Prestemon S O, Sabbi G and Scalan R M 2007 *IEEE Trans. Appl. Supercond.* **17** 1149–52

[6] See for example a comparative plot by Lee P J online at: http://magnet.fsu.edu/∼lee/plot/plot.htm

[7] Collings E W, Sumption M D, Scanlan R M, Dietderich D R, Motowidlo L R, Sokolowski R S, Aoki Y and Hasegawa T 1999 *Supercond. Sci. Technol.* **12** 87–96

[8] Motowidlo L R, Sokolowski R S, Hasegawa T, Aoki Y, Koizumi T, Ohtani N, Scanlan R, Dietderich D and Nagaya S 2000 *Physica* C **341–348** 2539–43

[9] Godeke A *et al* 2010 *Supercond. Sci. Technol.* **23** 034022

[10] Ekin J W, Finnemore D K, Li Q, Tenbrink J and Carter W 1992 *Appl. Phys. Lett.* **61** 858–60

[11] Kuroda T, Yuyama M, Itoh K and Wada H 1992 *Adv. Cryog. Eng.* **38** 1045–51

[12] ten Haken B and ten Kate H H J 1995 *IEEE Trans. Appl. Supercond.* **5** 1298–301

[13] Wesche R, Fuchs A M, Jakob B and Pasztor G 1996 *Cryogenics* **36** 419–26

[14] ten Haken B, Godeke A, Schuver H J and ten Kate H H J 1996 *IEEE Trans. Magn.* **32** 2720–3

[15] ten Haken B and ten Kate H H J 1996 *Physica* C **270** 21–4

[16] ten Haken B, Beuink A and ten Kate H H J 1997 *IEEE Trans. Appl. Supercond.* **7** 2034–7

[17] Sugano M and Osamura K 2004 *Physica* C **402** 341–6

[18] Osamura K, Sugano M and Matsumoto K 2003 *Supercond. Sci. Technol.* **16** 971–5

[19] Marken K R, Miao H, Meinesz M, Czabaj B and Hong S 2003 *IEEE Trans. Appl. Supercond.* **13** 3335–38

[20] Heine K, Tenbrink J and Thöner M 1989 *Appl. Phys. Lett.* **55** 2441–2443

[21] Shen T, Jiang J, Yamamoto A, Trociewitz U P, Schwartz J, Hellstrom E E and Larbalestier D C 2009 *Appl. Phys. Lett.* **95** 152516

[22] Shen T, Jiang J, Kametani F, Trociewitz U P, Larbalestier D C, Schwartz J and Hellstrom E E 2010 *Supercond. Sci. Technol.* **23** 025009

[23] Walters C R, Davidson I M and Tuck G E 1986 *Cryogenics* **26** 406–12

[24] Cheggour N and Hampshire D P 2000 *Rev. Sci. Instrum.* **71** 4521–30

[25] Sugano M, Itoh K and Kiyoshi T 2006 *IEEE Trans. Appl. Supercond.* **16** 1039–42

[26] Lu X F, Cheggour N, Stauffer T C, Clickner C C, Goodrich L F, Trociewitz U, Myers D and Holesinger T G 2011 *IEEE Trans. Appl. Supercond.* **21** 3086–9

[27] Matsumoto A, Kitaguchi H, Kumakura H, Nishioka J and Hasegawa T 2004 *Supercond. Sci. Technol.* **17** 989–92

[28] Hasegawa T, Koizumi T, Hikichi Y, Nakatsu T, Scanlan R M, Hirano N and Nagaya S 2002 *IEEE Trans. Appl. Supercond.* **12** 1136–40

[29] Miao H, Marken K R, Meinesz M, Czabaj B, Hong S, Rikel M O and Bock J 2006 *Adv. Cryog. Eng.* **52** 673–82

[30] Huang Y K, ten Haken B and ten Kate H H J 1999 *IEEE Trans. Appl. Supercond.* **9** 2702–5

[31] Passerini R, Dhallé M, Seeber B and Flükiger R 2002 *Supercond. Sci. Technol.* **15** 1507–11

[32] van der Laan D C, Schwartz J, ten Haken B and Dhallé M 2008 *Phys. Rev.* B **77** 104514

[33] Sunwong P, Higgins J S and Hampshire D P 2011 *IEEE Trans. Appl. Supercond.* **21** 2840–4

[34] Koizumi T, Hasegawa T, Nishioka J, Hikichi Y, Nakatsu T, Kumakura H, Kitaguchi H, Matsumoto A and Nagaya S 2005 *IEEE Trans. Appl. Supercond.* **15** 2538–41

[35] Holesinger T G, Johnson J M, Coulter J Y, Safar H, Phillips D S, Bingert J F, Bingham B L, Maley M P, Smith J L and Peterson D E 1995 *Physica* C **253** 182–90

[36] Rikel M O, Wesolowski D, Yuan Y and Hellstrom E E 2001 *Physica* C **354** 321–6

[37] Holesinger T G, Kennison J A, Marken K R, Miao H, Meinesz M and Campbell S 2005 *IEEE Trans. Appl. Supercond.* **15** 2562–65

[38] Kametani F *et al* 2011 *Supercond. Sci. Technol.* **24** 075009

[39] Holesinger T G *et al* 2005 *IEEE Trans. Appl. Supercond.* **15** 2514–17

[40] Cheggour N, Ekin J W, Clickner C C, Verebelyi D T, Thieme C L H, Feenstra R and Goyal A 2003 *Appl. Phys. Lett.* **83** 4223–5

[41] Cheggour N, Ekin J W, Xie Y-Y, Selvamanickam V, Thieme C L H and Verebelyi D T 2005 *Appl. Phys. Lett.* **87** 212505

[42] Cheggour N, Ekin J W and Thieme C L H 2005 *IEEE Trans. Appl. Supercond.* **15** 3577–80

[43] Cheggour N, Ekin J W, Thieme C L H, Xie Y-Y, Selvamanickam V and Feenstra R 2005 *Supercond. Sci. Technol.* **18** S319–24

[44] Sugano M, Osamura K, Prusseit W, Semerad R, Kuroda T, Itoh K and Kiyoshi T 2005 *IEEE Trans. Appl. Supercond.* **15** 1136–40

[45] van der Laan D C and Ekin J W 2007 *Appl. Phys. Lett.* **90** 052506

[46] van der Laan D C, Douglas J F, Clickner C C, Stauffer T C, Goodrich L F and van Eck H J N 2011 *Supercond. Sci. Technol.* **24** 032001

[47] van Eck H J N, Vargas L, ten Haken B and ten Kate H H J 2002 *Supercond. Sci. Technol.* **15** 1213–5

[48] Chen X-F, Tessema G X and Skove M J 1991 *Physica* C **181** 340–4

[49] Watanabe N, Fukamachi K, Ueda Y, Tsushima K, Balbashov A M, Nakanishi T and Mori N 1994 *Physica* C **235–240** 1309–10

[50] Meingast C, Junod A and Walker E 1996 *Physica* C **272** 106–14

[51] Ekin J W 1980 *Cryogenics* **20** 611–24

[52] Welch D O 1980 *Adv. Cryog. Eng.* **26** 48–65

[53] Keys S A, Koizumi N and Hampshire D P 2002 *Supercond. Sci. Technol.* **15** 991–1010

[54] Dhallé M, van Weeren H, Wessel S, den Ouden A, ten Kate H H J, Hušek I, Kováč P, Schlachter S and Goldacker W 2005 *Supercond. Sci. Technol.* **18** S253–60

[55] Cheggour N and Hampshire D P 2002 *Cryogenics* **42** 299–309

[56] Jiang J, Starch W L, Hannion M, Kametani F, Trociewitz U P, Hellstrom E E and Larbalestier D C 2011 *Supercond. Sci. Technol.* **24** 082001

[57] Jiang J *et al Presentation at the ICMC Conf. (Spokane, Washington, June 2011)*

[58] Mbaruku A L, Le Q V, Song H and Schwartz J 2010 *Supercond. Sci. Technol.* **23** 115014